# Predictive MPPT AI algorithm for fast response during tumbling conditions

Gaia Lorenzi
Department of Mechanical and Aerospace Engineering,
Sapienza Università di Roma
Rome, Italy
gaia.lorenzi@uniroma1.it

Enrico Dalmo
N.P.C New Production Concept S.r.l. - SPACEMIND
Imola, Italy
e.dalmo@npcitaly.com

Chiara Lughi
N.P.C New Production Concept S.r.l. - SPACEMIND
Imola, Italy
c.lughi@npcitaly.com

Damiano Accurso
N.P.C New Production Concept S.r.l. - SPACEMIND
Imola, Italy
d.accurso@npcitaly.com

Fabrizio Piergentili
Department of Mechanical and Aerospace Engineering,
Sapienza Università di Roma
Rome, Italy
fabrizio.piergentili@uniroma1.it

***Abstract*— Efficient power harvesting for small satellites is critical for mission success, especially during the initial detumbling phase and in case of attitude control anomalies. In these scenarios, the illumination conditions of the solar panels can vary at high frequency, and conventional Maximum Power Point Tracking (MPPT) techniques may struggle to reach a point of good power conversion under fast transients. If detumbling issues arise and cannot be promptly resolved, the batteries may discharge before ground intervention is possible, leading to the loss of the spacecraft and an early end of the mission.**

**In this work, we introduce a novel MPPT approach based on onboard artificial intelligence. The method adapts continuously to the spacecraft's electrical and environmental conditions with real-time telemetry from the photovoltaic modules as input. By predicting short-term trends in illumination and electrical behavior, the controller is capable of anticipating cycling changes and adjusting the duty cycle proactively, rather than only reacting as happens with a standard Perturb and Observe method.**

**Since the controller adapts autonomously to onboard telemetry rather than relying on mission-specific datasets, it can be integrated into different spacecraft and photovoltaic configurations without extensive tuning or characterization before launch. The approach reduces the amount of power that would otherwise be lost during tumbling, deployment, or attitude disturbances. By maintaining a more favorable operating point under non-stationary conditions, the system helps preserve power availability during critical mission phases.**

**Early simulation results support the feasibility of the approach and demonstrate potential advantages in maintaining a fast reaching of the point of maximum power in cycling conditions of illumination, particularly during tumbling and post-deployment phases. The simulation results show the potential of AI-assisted power management for future technological development, suggesting that intelligent control can be integrated into power electronics without compromising safety or resource constraints.**

**Keywords— MPPT, Power System, EPS, Solar panels, AI**

## I. INTRODUCTION

In the context of the new space economy, small satellites are increasingly being developed to host high-performance payloads within reduced form factors. In these satellites, the primary source of energy is solar power, with solar cells achieving efficiencies of up to 34%.

To fully exploit the available solar power, the satellite's Electrical Power Subsystem (EPS) must manage energy efficiently throughout all phases of the mission, including the initial detumbling phase. In particular, it is crucial that the Maximum Power Point Tracking (MPPT) system is able to track the maximum power point as accurately as possible, especially during critical phases when the available power is limited.

During a nominal CubeSat deployment, the rotation rate is typically below 45 °/s [1] [2], but release anomalies may occur, resulting in an initial tumbling rate higher than nominal, at 100 °/s or higher [2]. Due to the rapid variation in illumination across the solar panels, an MPPT based on a classical perturb-and-observe algorithm may fail to extract sufficient energy from the panels, potentially leading to mission loss caused by battery depletion before the completion of the detumbling phase.

To address this issue and improve the efficiency of maximum power point tracking, this paper investigates the possibility of employing an alternative MPPT algorithm to the classical perturb-and-observe approach, based on artificial intelligence. Such algorithms have already been explored for terrestrial applications, where they are also used to adapt to and predict irradiance variations based on weather forecasting [3], [4], [5].

In space environment, these approaches have been investigated under nominal conditions, including for CubeSats [6], [7], [8]. However, some Artificial Neural Network (ANN)–based algorithms that require training have shown performance degradation as solar cells age, compared to Beginning-of-Life (BOL) conditions, resulting in reduced efficiency relative to classical methods [9].

The objective of this paper is to present the development of a neural network that not only reacts but also predicts and anticipates the variation of the optimal duty cycle at the next step, based on the recognition of the cyclic pattern of irradiance during detumbling phases, while maintaining efficiency in subsequent mission phases. This approach enables higher power extraction throughout the mission and provides a fail-safe capability in the event of incorrect deployment, supporting satellite recovery.

The results obtained with the neural network–based algorithm were compared against the corresponding ideal duty cycle values and those achieved using a classical perturb-and-observe approach, for three different initial tumbling rate scenarios.

## II. NEURAL NETWORK IMPLEMENTATION

To achieve the objective of rapidly identifying and maintaining the maximum power point during the detumbling phase, as well as throughout the mission, an algorithm based on a feedforward neural network has been developed. This network is designed to predict the evolution of irradiance curves based on input data acquired from sensors mounted on the solar panels. In particular, irradiance and temperature can be derived from photodiodes and NTC thermistors installed on the panel surface; therefore, in the simulation, these quantities are treated as known inputs representing the current state of the panel.

The network is trained online during the simulation to enable its applicability to different types of solar cells and to prevent performance degradation associated with cell aging. Since the network does not require prior training, it ensures adaptability to any power system configuration and to the specific solar cell technology used.

The network is trained using a gradient descent algorithm with momentum. In this formulation, the weight update is based on the gradient of the error with respect to the simulation step, while the momentum term acts as a form of infinite impulse response (IIR) filter over the gradients, smoothing the update trajectory and improving convergence stability.

To enhance numerical stability and prevent drift or divergence during training, a normalization procedure is applied to the input data and/or gradient signals. In addition, a replay memory mechanism with prioritized sampling is introduced. This strategy preferentially selects training samples associated with higher prediction errors, as these samples carry more informative content for learning.

The neural network controller then performs a form of local predictive correction by evaluating multiple candidate duty cycle values and selecting the one that maximizes the estimated power output. This selection process incorporates penalty terms that account for abrupt or excessively large variations in the duty cycle. This introduces an implicit filtering effect, which reduces high ripple by penalizing candidate solutions that would lead to significant changes in the subsequent duty cycle, while still permitting large adjustments when they yield a clear improvement in performance.

The algorithm incorporates either adaptive step-size updates or a hold mechanism, whereby the previously selected duty cycle is maintained when it is already close to optimal. This helps reduce unnecessary switching and improves steady-state stability.

To mitigate the risk of convergence to local minima, an escape strategy is implemented. When the duty cycle remains below a predefined threshold for three consecutive samples, the algorithm initiates a broader exploration of the search space by considering larger duty cycle variations, thereby increasing the likelihood of recovering from suboptimal operating points.

To test the performance and demonstrate the efficiency of the neural network, simulations were conducted considering a 3U-sized CubeSat configuration in a LEO sun synchronous orbit at 550km of altitude. A constant power consumption of 3.5 W was assumed for the spacecraft platform subsystems during the detumbling phase. The B-dot control algorithm is simulated using 3 magnetorquers with the following characteristic: a magnetic dipole moment of $A \cdot m^2 = 0.35$, a number of coil turns $N = 93$, an effective coil area of $0.0075\ \mathrm{m}^2$, and a maximum current $I_{\max} = 0.5$ A.

Three different scenarios are presented, for a nominal deployment case at 20°/s, an intermediate scenario of 45°/s, and an anomalous high-rate deployment case at 100°/s. For each scenario, 50 simulations were performed in order to obtain a statistically meaningful estimate of the algorithm's average performance and response efficiency.

For each case, efficiency plots will be presented and compared with those obtained using a classical perturb-and-observe algorithm. In addition, the duty cycle evolution during the detumbling phases will be shown for both approaches, along with a comparison against the ideal duty cycle profile.

The temperature of the solar cells varies in orbit due to changing illumination conditions, which also affects the power extracted from the solar arrays. During a standard detumbling phase, the solar panels can experience temperature fluctuations approximately ranging from −20°C to +25°C [10]. However, these values depend on several factors, including the type of orbit (and thus the duration of eclipse and sunlight periods) as well as the material properties of the solar panel substrate. To isolate the neural network's response to irradiance variations, the simulations were performed assuming a constant temperature of 25°C.

The I–V curve of the solar cells used for the simulations was reconstructed using a four-parameter approach based on the characteristic points $I_{sc}, V_{oc}, I_{mpp}, V_{mpp}$, as commonly adopted in empirical photovoltaic modeling [11] [12]. The model provides a simplified yet effective representation of the solar cell behavior, suitable for system-level simulations.

Fig. 1 shows the model compared with the I–V curve of a triple-junction solar cell at 25°C.

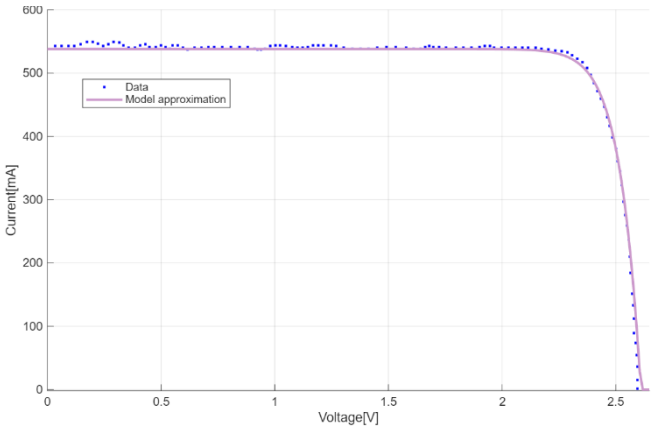



Fig. 1 Solar cell model used for simulations

## III. SCENARIO 1: 20°/SEC

This scenario corresponds to the lowest rotational rate considered, and 50 simulations were performed under identical initial conditions. As shown in the plot in Fig. 2 of one of the simulations, the MPPT implemented using the ANN-based algorithm is more efficient than the perturb-and-observe approach, achieving an average efficiency of 98.07% and a minimum efficiency of 97.47% across the simulations, compared to an efficiency of 95.1% obtained with the perturb-and-observe method.

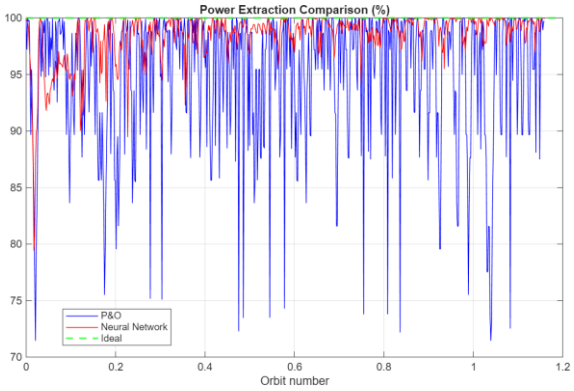



Fig. 2 Power extraction comparison for detumbling with 20°/s initial velocity

Fig. 3 shows an example of how the optimal duty cycle is set by the two algorithms compared to the ideal duty cycle for one of the simulations. It can be observed that the duty cycle predicted by the ANN exhibits lower initial overshoot and remains closer to the ideal value throughout the entire detumbling phase.

Fig. 4 shows the deviation from the mean of the power extraction efficiency across the 50 simulations performed under initial rotational conditions of 20°/s. A maximum deviation of 0.58% from the mean can be observed, indicating that the neural network exhibits a robust and consistent behavior across multiple test cases.

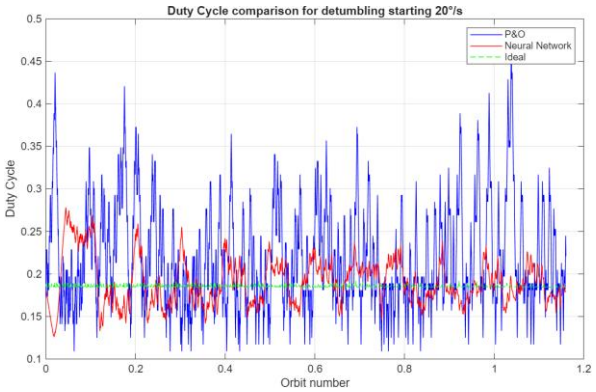



Fig. 3 Duty cycle comparison for detumbling with 20°/s initial velocity

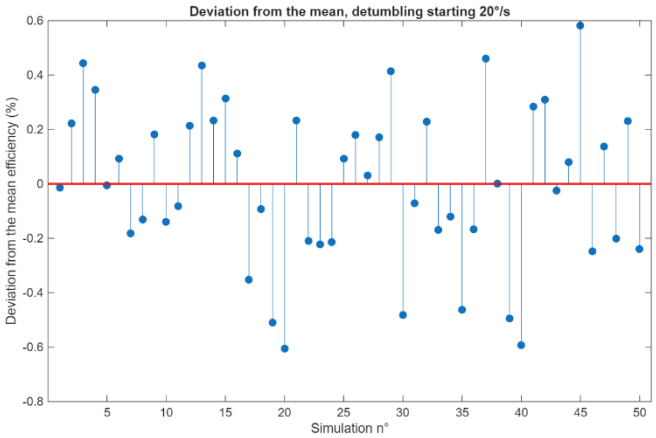



Fig. 4 Deviation from the mean for 50 simulations, starting 20°/s

## IV. SCENARIO 2: 45°/SEC

For the second detumbling scenario, with an initial rotational rate of 45°/s, 50 simulations were also performed under the same initial conditions. In this case, an average power extraction efficiency of 98.76% was achieved, with a minimum efficiency of 98.37% for the worst case.

It can be observed that the neural network maintains its performance close to the ideal value, progressively improving over time, whereas the perturb-and-observe algorithm exhibits a more consistent but less optimal behavior, characterized by noticeable spikes, with an efficiency of 94.67%. The power extraction efficiency of one of the simulation is shown in Fig. 5.

Fig. 6 shows the evolution of the duty cycle set by the two MPPT algorithms in one of the 50 simulations with an initial rotational rate of 45°/s. It can be observed that the ANN-based algorithm deviates significantly less from the ideal duty cycle compared to the classical perturb-and-observe method, thereby explaining the improved power extraction performance.

Fig. 7 presents the deviation from the mean efficiency values across the 50 simulations. It can be seen that the maximum deviation, in absolute terms, is lower than in the previous case, amounting to −0.39%.

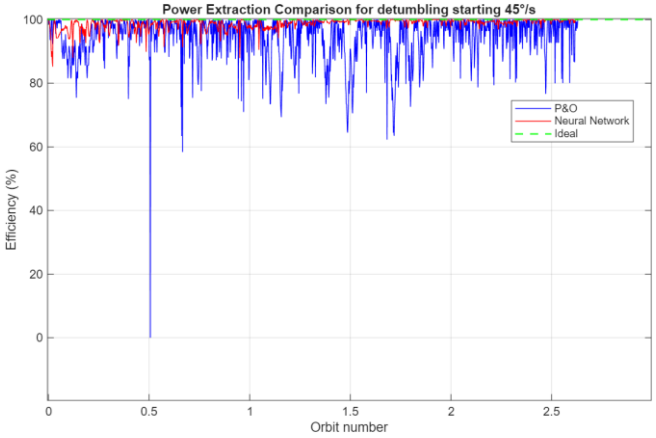



Fig. 5 Power extraction comparison for detumbling with 45°/s initial velocity

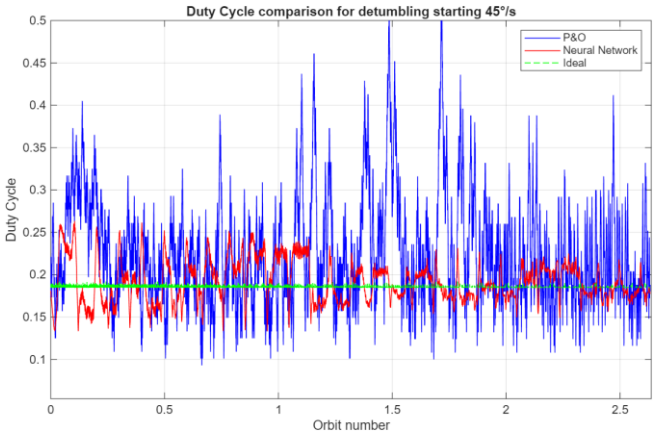



Fig. 6 Duty cycle comparison for detumbling with 45°/s initial velocity

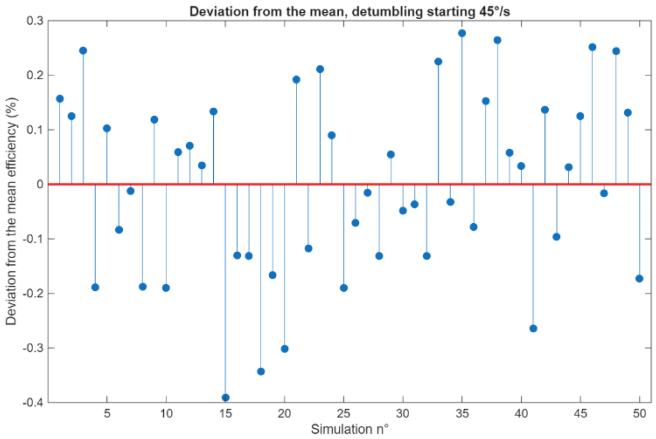



Fig. 7 Deviation from the mean for 50 simulations, starting 45°/s

## V. SCENARIO 3: 100°/SEC

For the most demanding case, with an initial rotational rate of 100°/s, the power extraction efficiency results are shown in Fig. 8. As clearly visible in the plot, the perturb-and-observe algorithm exhibits large spikes that persist throughout the entire detumbling phase, whereas the ANN-based algorithm, after an initial learning phase, follows the ideal power profile in a near-optimal manner.

Fig. 9 shows a zoomed-in view of the region between orbit 2 and 3, where the difference in response between the two algorithms is particularly evident. The ANN-based algorithm achieves an average power extraction efficiency of 99.33%, with a minimum of 99.00%, significantly higher than that obtained with the perturb-and-observe approach, which reaches 93.87%.

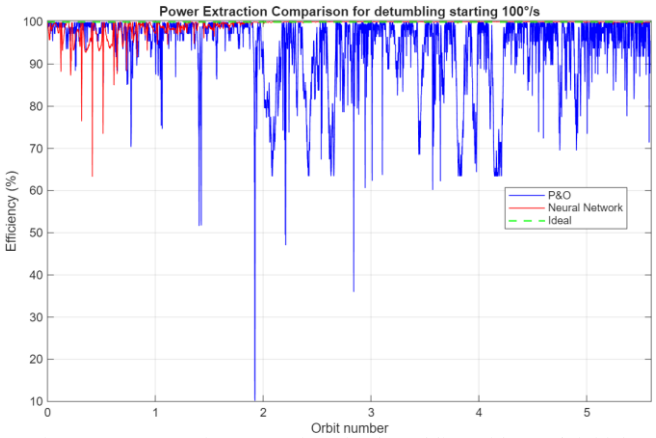



Fig. 8 Power extraction comparison for detumbling with 100°/s initial velocity

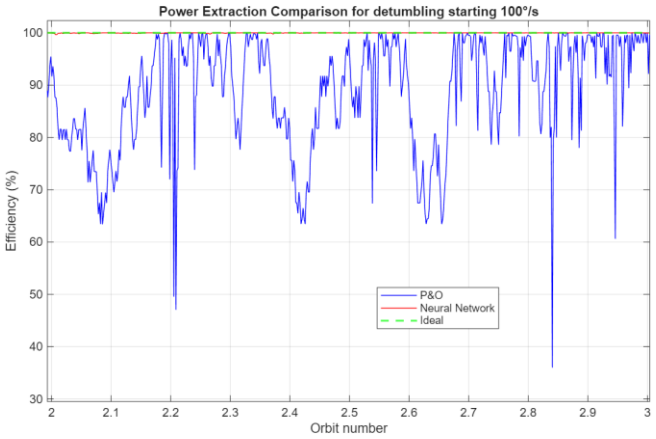



Fig. 9 Detail of power extraction efficiency, 100°/s

In Fig. 10, it is shown that the duty cycle determined by the neural network is significantly more accurate than that predicted by the perturb-and-observe method, particularly in the orbits following the second, where the latter almost completely loses the operating point.

The deviation from the mean efficiency across the 50 simulations, shown in Fig. 11, is even lower in absolute value compared to the previous cases, amounting to −0.34%.

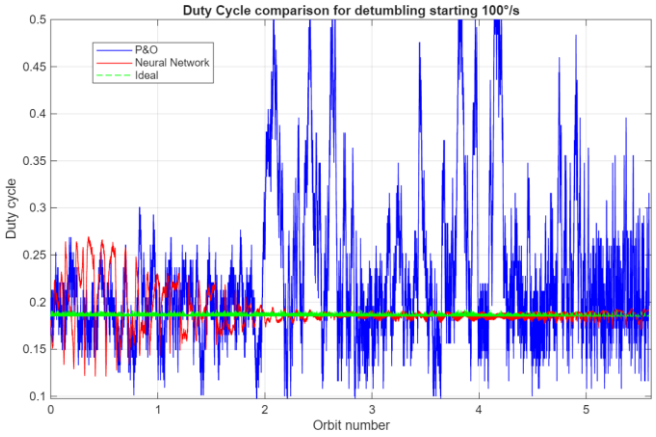



Fig. 10 Duty cycle comparison for detumbling with 100°/s initial velocity

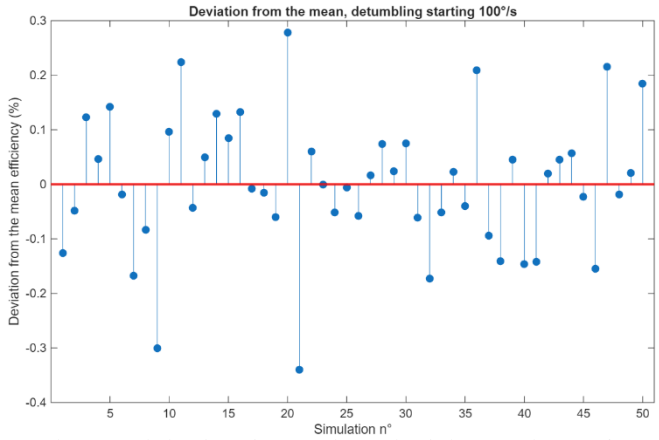


Fig. 11 Deviation from the mean for 50 simulations, starting 100°/s

## VI. RESULTS DISCUSSION

The results obtained from the three simulation scenarios demonstrate that, in the cases considered, the neural network achieves higher efficiencies than the perturb-and-observe algorithm. In particular, the ANN-based approach starts with superior efficiency under nominal detumbling conditions and even shows improved performance as the initial rotational rate increases, whereas the efficiency of the perturb-and-observe method decreases under the same conditions.

In particular, the ANN-based algorithm performs effectively both during the initial detumbling phase and in subsequent orbits, where it learns the rotational dynamics and is able to actively predict the duty cycle to be applied with high accuracy. This represents a significant advantage of ANN-based approaches, as algorithms lacking memory cannot achieve a comparable level of performance.

Fig. 12 summarizes the efficiency trends across the 50 simulations and highlights the consistency of the results over the different tests, clearly demonstrating the superior performance of the ANN-based approach. Table 1 provides a summary of the results in terms of average efficiency across the simulations conducted.

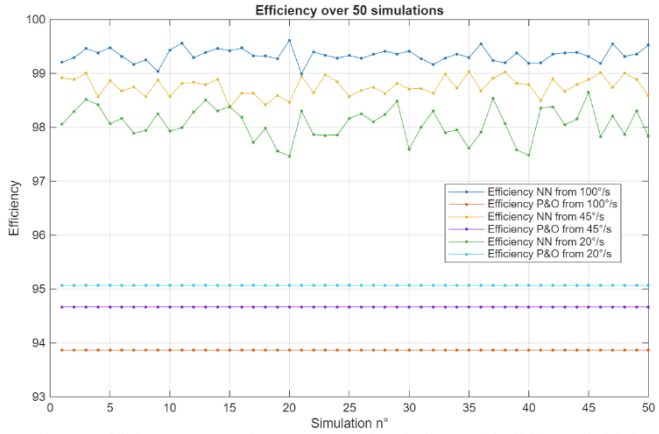


Fig. 12 Efficiency comparison over 50 simulations with different initial conditions

| | P&O | ANN |
|---|---|---|
| **Efficiency 20°/s (%)** | 95.1 | 98.07 |
| **Efficiency 45°/s (%)** | 94.67 | 98.76 |
| **Efficiency 100°/s (%)** | 93.87 | 99.33 |

Table 1 Summary of the efficiency results obtained for the analyzed cases

## VII. CONCLUSIONS

This work demonstrates the feasibility of an ANN-based MPPT strategy for CubeSat applications, capable of improving power extraction efficiency during highly dynamic detumbling conditions without requiring prior offline training. An ANN-based MPPT algorithm was developed and applied to a 3U CubeSat in a scenario of a LEO SSO 550km orbit. The neural network is based on a prediction of the optimal duty cycle and does not require prior training for its operation.

Several simulations were carried out considering initial tumbling rates at deployment of 20°/s, 45°/s, and 100°/s. For each case, 50 simulations were performed under identical initial conditions to validate the algorithm.

The results were compared with those obtained using a classical perturb-and-observe (P&O) algorithm applied to the same scenarios, demonstrating improved power extraction efficiency in all three cases. In particular, the neural network is able to learn from the observed dynamics and apply this knowledge, significantly enhancing efficiency even in cases where the detumbling phase requires a long duration, such as the worst-case scenario at 100°/s. The ability of the neural network to implicitly learn and exploit the dynamical evolution of the system during detumbling represents a key advantage over memoryless classical MPPT methods.

For the simulations, a constant temperature of 25°C and an ideal model of sensors was assumed in order to isolate the algorithm's response to irradiance variations. The next implementation will consider temperature variations on the solar cell, allowing the corresponding changes in the cell I–V characteristics to be taken into account and enabling an analysis of the algorithm's response under more realistic conditions

Subsequently, the algorithm will be tested on a real MPPT hardware platform within a test bench environment, using a solar simulator and an EPS emulation setup, in order to validate the results for potential future in-orbit application. . Since the simulations do not account for measurement and sensor noise, real measurements will be used to validate the algorithm's real-time response.

## REFERENCES

[1] J. C. Springmann, B. P. Kempke, J. W. Cutler, and H. Bahcivan, "Initial Flight Results of the RAX-2 Satellite".

[2] I. Gavrilovich, "Development of a robotic system for CubeSat Attitude Determination and Control System ground tests," 2016, [Online]. Available: NNT : 2016MONTT329. tel-01816985

[3] M. Jlidi, O. Barambones, F. Hamidi, and M. Aoun, "ANN for Temperature and Irradiation Prediction and Maximum Power Point Tracking Using MRP-SMC," *Energies*, vol. 17, no. 12, p. 2802, Jun. 2024, doi: 10.3390/en17122802.

[4] M. Gupta, A. Arya, U. Varshney, J. Mittal, and A. Tomar, "A review of PV power forecasting using machine learning techniques," *Prog. Eng. Sci.*, vol. 2, no. 1, p. 100058, Mar. 2025, doi: 10.1016/j.pes.2025.100058.

[5] P. Agrawal, H. O. Bansal, A. R. Gautam, O. P. Mahela, and B. Khan, "Transformer-based time series prediction of the maximum power point for solar

photovoltaic cells," *Energy Sci. Eng.*, vol. 10, no. 9, pp. 3397–3410, Sep. 2022, doi: 10.1002/ese3.1226.

[6] S. Noroozi, H. Shayanfar, and M. Nasirian, "Design of an intelligent MPPT for a PV array mounted on a satellite considering outer space," *Int. Trans. Electr. Energy Syst.*, vol. 31, no. 9, Sep. 2021, doi: 10.1002/2050-7038.12984.

[7] M. Attalla, R. El-Sehiemy, and H. El-Arwash, "A Fuzzy Logic Based Maximum Power Point Tracking of PV Systems Supplying Remote Sensing Devices of Two Units Cube Satellite Applications," *ERJ Eng. Res. J.*, vol. 0, no. 0, pp. 0–0, Apr. 2024, doi: 10.21608/erjm.2024.263628.1315.

[8] A. Abagero, Y. Abebe, A. Tullu, Y. S. Jung, and S. Jung, "Deep Learning-Based MPPT Approach to Enhance CubeSat Power Generation," *IEEE Access*, vol. 13, pp. 40076–40089, 2025, doi: 10.1109/ACCESS.2025.3546066.

[9] M. Kermadi and E. M. Berkouk, "Artificial intelligence-based maximum power point tracking controllers for Photovoltaic systems: Comparative study," *Renew. Sustain. Energy Rev.*, vol. 69, pp. 369–386, Mar. 2017, doi: 10.1016/j.rser.2016.11.125.

[10] A. Pál *et al.*, "GRBAlpha: The smallest astrophysical space observatory: I. Detector design, system description, and satellite operations," *Astron. Astrophys.*, vol. 677, p. A40, Sep. 2023, doi: 10.1051/0004-6361/202346182.

[11] M. G. Villalva, J. R. Gazoli, and E. R. Filho, "Comprehensive Approach to Modeling and Simulation of Photovoltaic Arrays," *IEEE Trans. Power Electron.*, vol. 24, no. 5, pp. 1198–1208, May 2009, doi: 10.1109/TPEL.2009.2013862.

[12] J. Kratochvil, W. Boyson, and D. King, "Photovoltaic array performance model.," SAND2004-3535, 919131, Aug. 2004. doi: 10.2172/919131.